Application of a Deflagration Plasma Gun as a Space Propulsion Thruster

DAH YU CHENG*
University of Santa Clara, Santa Clara, Calif.

The application of the magnetized plasma deflagration process to space propulsion is introduced. The deflagration process has the unique capability of efficiently converting input energy into kinetic energy in the accelerating direction. Examples of the differences between deflagration and detonation are given, such as their current densities, their temperature, and their particle velocities. Magnetic field profiles of the two modes of discharges are measured. Preliminary temperature measuring technique is introduced. Specific impulses measured by piezoelectric probe and pendulum methods are presented. The influence of the transmission line in the discharge circuits on that of plasma velocity is measured by means of microwave time-of-flight method. The results for the deflagration gun are compared with other space thrusters.

I. Introduction

WHEN space exploration extends beyond the moon, a high specific impulse thruster is very desirable if the thruster can also produce high enough thrust densities. Chemical rockets have high thrust density but not high enough specific impulse. Ion engines have high specific impulse but not high enough thrust density. A plasma gun operated in the deflagrational mode of discharge originally designed for nuclear fusion experiments has demonstrated both high specific impulse and high thrust density capability suitable for space travel.

The dimensions of the gun are shown in Fig. 1. The gun has two anode configurations, a straight barrel and a 3° tapered barrel. The historical development and the focusing property are given in detail in Ref. 1. The capability of focusing the plasma may not be of any use for a space thruster, but it facilitates the plasma property measurements in laboratories. The properties of the deflagration gun that are suitable for a space propulsion device are presented here. The concept of the deflagration discharge will be reviewed. Demonstration of the differences between deflagration and detonation can be shown by measuring the magnetic field profiles in the discharge zone. Low-static temperature of the flowing plasma is recorded by a vacuum ultraviolet spectrograph. Impact pressures of the plasma stream as a function of capacitor bank voltage and energy are obtained by piezoelectric probes. Impact pressure was also obtained by a fish-trap pendulum. Transmission lines were added to the capacitor bank, after which the velocities of plasma were measured by the time-of-flight method using two sets of microwave transmission and receiving horns. The gun demonstrates its versatility to produce a wider range of specific impulse than other devices. Comparisons of specific impulses and thrusts with other existing devices were also made.

Received November 16, 1970; revision received May 10, 1971. This work is partially supported by NASA University Grant 05-017-019, under a cooperative program with the High-Enthalpy Research Branch, NASA Ames Research Center, Moffett Field, Calif. The author would like to express his sincere thanks to H. A. Stine, of the HER Branch, NASA Ames Research Center, for his support and cooperation of this work. Without G. Giorgetti, S. Kost, F. Baker, and A. Somes, the experimental work would have been impossible to carry out. The author wants to give his greatest appreciation to all of them.

Index Categories: Electrical and Advanced Space Propulsion; Plasma Dynamics and MHD; Spacecraft Propulsion Systems Integrations.

* Associate Professor, Mechanical Engineering Department. Member AIAA.

II. A Brief Review of the Deflagration Theory

Deflagration and detonation theory was thoroughly studied in the field of combustion.[2] In short, when energy is added to a flowing stream, two possible equilibrium conditions exist; namely, by heating and compression or by heating and expansion. The equilibrium conditions are determined by the entropy extrema of the process. In the compression case, it is called Chapman-Jouquet detonation and in the expansion case, it is called Chapman-Jouquet deflagration. If the magnetohydrodynamic Bernoulli equation[3] is used together with the concepts of total pressure P^* and total temperature T^* (Ref. 1), then the Chapman-Jouquet conditions for detonation and deflagration also exist for a magnetized plasma. The equilibrium states can be expressed in a dimensionless P^*, τ diagram as shown in Fig. 2. The original state is located at (1,1). The tangent from the point (1,1) to two sides of a fixed energy jump ($H = 3$) represents the Chapman-Jouquet detonation and deflagration. Constant nondimensional temperatures and constant entropy curves are also shown for comparison. The total pressure P^* is defined as a sum of the particle pressure p, and the magnetic pressure $B^2/8\pi$, and the nondimensional H is defined as energy addition per unit mass divided by the total internal energy at the state (1,1); therefore, ($H = 0$) corresponds to no energy

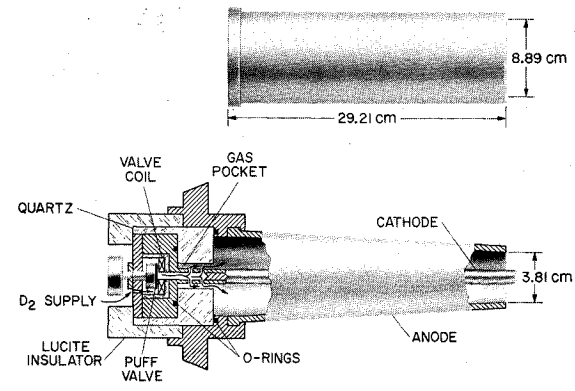

Fig. 1 Deflagration plasma gun with two anode configurations.

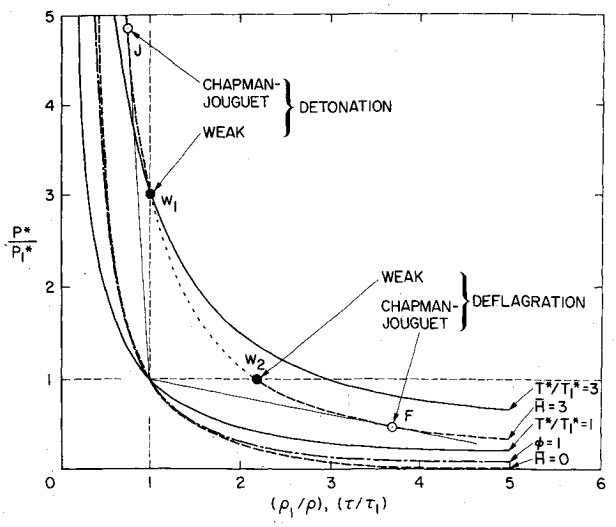

Fig. 2 $P^*\tau$ diagram for detonation and deflagration processed in plasmas.

addition. For the detonation condition on the $H = 3$ curve, one can see that the total pressure P^* increases by a factor of 5 and that the density ratio increases by 20% and that the temperature jumped by a factor of more than 3. These effects indicate a possible severe energy loss by heat radiation. In contrast, the deflagration point F on the same curve has a nondimensional total pressure drop by a factor of 4, a density decrease by a factor of 3.8 and a temperature ratio increase only by about 1.5. With a fixed amount of energy input, the heat loss in the detonation case is obviously much larger than that of the deflagration case. The decrease in density means a rapid increase in particle velocity as a consequence of the mass conservation law. The smaller temperature increase with fixed energy input indicates the deflagration process is very efficient means to accelerate plasma particles, whereas the detonation process is a very efficient means for plasma heating.[4]

To operate in a deflagration mode, a good vacuum is required, which is the condition for outer space. To obtain deflagration discharge in the plasma gun the gun chamber is first evacuated to a hard vacuum condition ($<10^{-6}$ torr). A 60 μF, 20 kv capacitor bank is connected to the gun without switches. The discharge is triggered by a fast open-and-close valve, which supplies gas into the spacing between the gun electrodes. The electrical discharge occurs on the vacuum side of the Paschen breakdown curve.[5] A sudden increase of gas density will lower the Paschen's critical breakdown voltage below that of the capacitor bank, causing the discharge to take place. Unlike the detonation discharge, the plasma can accelerate out of the gun nozzle unimpeded by collisions with neutral gas. The discharge zone is usually very thick. Similar properties were found in quasi-steady discharges at lower current level of Ref. 6. The ionization front propagates back towards the gun breech to ionize the on-coming neutral gases particles.

A magnetic probe was used to map the time history of the magnetic field profile inside the gun barrel, as presented in Figs. 3a and 3b. The dimension of the gun and the probe location are shown on the top of Fig. 3a. A set of oscillograph traces of probe signals at various axial locations is shown at the bottom. Deflagration field profiles are displayed from the breakdown time to 8 μsec later. After the current reverses its direction, some neutral gases are present in the gun barrel, causing a detonation discharge to form. The resulting shock front accompanied by the abrupt jump in magnetic field intensity shown after 8 μsec. The relatively constant magnetic field in the detonation case is due to the nature of its thin discharge current sheet. On the other hand, the deflagration discharge has much higher total current and energy transfer rate to the plasma, so the thick discharge current zone will have a current density smaller than that of the detonation case. It is also known[4] that the moving snowplow current sheet does not accelerate particles at the gun muzzle; instead a pinch is formed at the tip of the center electrode. If the tip is hollow, some of the plasma actually accelerates backward into the hollow center electrode.

III. Temperature Measurement

In a pinched-plasma gun, the plasma temperature frequently reached from 1 kev to over 10 kev. The expansion process of the deflagration discharge would be efficient if the plasma temperature were low. The rest of the energy then could be used to accelerate the plasma. To measure the plasma stream temperature, a $\frac{1}{2}$ m McPherson vacuum ultraviolet spectrograph is used. If the stream temperature is not as high as the detonation discharge, the Bremmstrahlung radiation cutoff may be well within the range of a Seya-Namioka mount spectrograph. The Bremmstrahlung cutoff has two distinct features; that it is a continuum radiation before cutoff, and that the cutoff is extremely rapid.[7] In this case, the grating efficiency does not have to be known. The cutoff wave length alone can provide information on plasma temperature. The grating used in the spectrograph is blazed at 800 Å with 28.3 Å/mm dispersion. The radiation is recorded on Kodak SWR film starting from the slit image. The plasma is viewed by the spectrograph from a 90° angle without windows. Hard vacuum is maintained both in spectrograph and the vacuum chamber (see Fig. 4). The cutoff wave length varies between firings from 185 Å to 210 Å. A typical densitometer trace is shown in Fig. 5. The cutoff at 210 Å gives a plasma temperature of 75 ev. This is very low in comparison with 1 kev to 10 kev produced by a pinch. The radiation is a continuum up to 450 Å before the first spectral line appears. From 210 Å to 450 Å is an interesting range for spectroscopic studies of the ionization process. This range fills the gap between the grazing incidence spectrograph and the hollow cathode light source for Seya-Namioka mount and other normal-incidence instruments.[8] The author attributes this radiation recording to the windowless, hard vacuum conditions between the plasma and the instrument. This can only be obtained in the deflagration mode of discharge.

IV. Impulse Measurement

The stagnation impulses are measured by piezoelectric probes and by a pendulum.[1,7,9] The piezoelectric cell is precalibrated by the manufacturer. The rise time of the cell is estimated to be 1 μsec. The sensing area is a $\frac{1}{4}$-in.-diam circle with an epoxy coating. For deuterium as a propellant, the impact pressures as a function of capacitor bank voltage and energy are shown in Fig. 6. The impulse increases with bank voltage but it is hard to distinguish this effect from that of increasing the storage energy. To distinguish the dependence on bank voltage from that of the storage energy, half of the capacitors were disconnected at 20 kv. The impulse showed an immediate drop by 40% at the same charged-bank voltage for stored energy of 3 kjoule.

When the stored capacitor energy is increased to 30 kjoule, a pendulum has to be used to measure the impact pressure. The pendulum arrangement is shown in Fig. 7. The plasma is injected upward and is focused by the 3° tapered anode at a point 10 in. away from the gun nozzle. The pendulum is suspended from the top of a glass vacuum chamber by a weak spring from a child's slinky toy. A T.V. camera and a video recorder were used during the firing. The maximum deflection can be obtained by playing back the recorded frames. The pendulum is made in the shape of a chinese fish trap, so

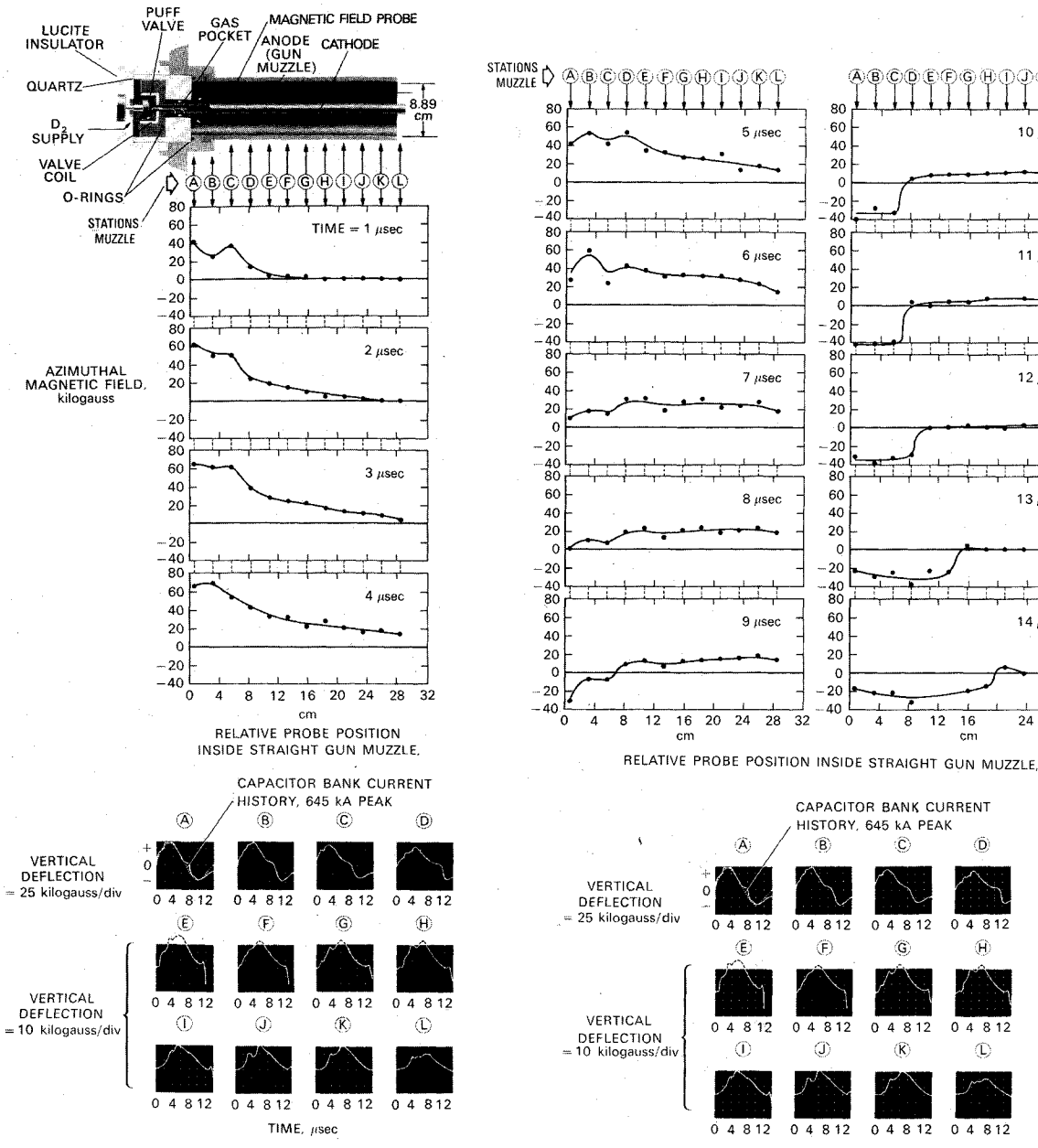

Fig. 3 Magnetic field profile and the formation of a detonation process.

the plasma could enter the front entrance and escape laterally through the perforated sides together with the ablated materials. Therefore, the momentum measured from the vertical deflection of the target will not contain components from the scattering of ablated materials. Argon propellant gas was used. The capacitor bank was charged to 15 kv, had a capacitance of 270 μf and an estimated inductance of 10 $\sim$ 15 nh. Again the gun is triggered by the propellant to obtain the deflagration discharge mode. Details of the fish trap configuration are shown in Fig. 8. The pendulum weighs 7 oz and has a pointed brass cone located at the end plate so the plasma would have to bounce off the wall before it could return through the entrance port.

One shot was made with this configuration, the pendulum being deflected upwards by $5\frac{1}{16}$ in. The damage resulting from the plasma impact is shown in Fig. 9. The pressure from the plasma is so high that the trap exploded and the brass end plate bent. It is felt that the impact is so severe that the plasma does not have a chance to escape from holes but must hit the side wall with most of its momentum. The metal wall bulged out as can be seen from Fig. 9. The accidental failure to the trap structure provided additional information. The metal properties of permanent strain are well known, so one can measure the distortion of the metal to estimate the impact pressure. After evaluating the impact

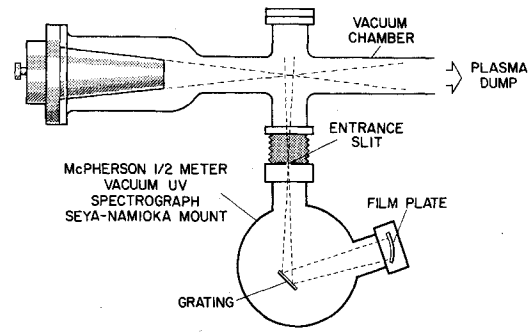

Fig. 4 Vacuum uv setup for spectrograph studies.

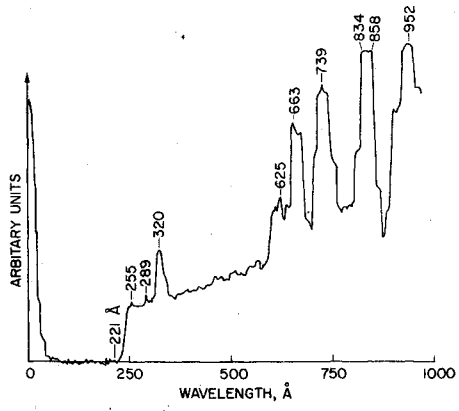

Fig. 5 Densitometer trace.

force from the vertical deflection using a spring constant of 0.335 oz/in., the total impact was calculated as 5837 lb or 2653 kg. This is based on a discharge time of 36 μsec. The actual direct target damage on the cone is about 1.5 cm in diameter. This yields an average impact pressure of 1502 kg/cm^2 or 21,329 psia. This concentration of pressure would not have happened if a straight anode had been used. This yields the average stagnation total pressure at the breech of

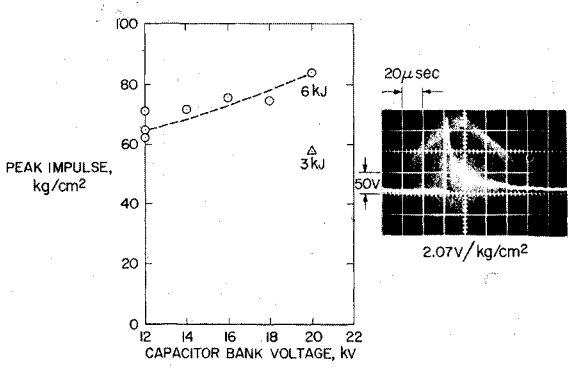

Fig. 6 Energy voltage relationship with impact pressure.

586 psia (42.6 kg/cm^2 = 4.20 × 10^{6}N/m^2). The velocity of argon for this shot was calculated from momentum and energy balance considerations to be 5.6 × 10^7 cm/sec. The mass of argon being processed was estimated to be 166 μg.

V. Time of Flight Velocity Measurement

The direct impulse measurement is important in that the actual impulse per discharge can be determined. The mass

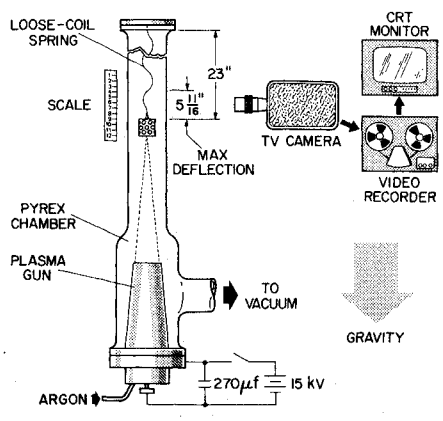

Fig. 7 Pendulum measurement setup.

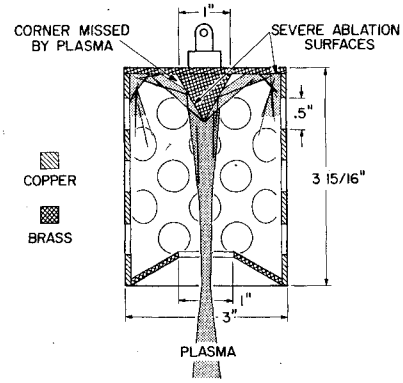

Fig. 8 A detail dimension of the fish trap pendulum.

and velocity in the measurement can be separated by momentum and energy equations if independent measurements can be made. A microwave time-of-flight arrangement is shown in Fig. 10. The transmission of the microwave can be cut off by the plasma front. When two sets of microwave transmission and receiving horns are located at a known fixed distance apart, the time delay on the cutoff signal determines the velocity of the plasma. The microwave signal is subject to three different problems—failure of cutoff at too low plasma density, poor time resolution at too high plasma speed, and bypassing of the plasma by the microwave beam if the plasma is focussed too sharply. However, it becomes an excellent tool when the plasma is slowed down for space thruster experiments. Due to the power-to-weight problem, the best thruster is not in the high specific impulse range. Transmission lines have been added to shape the discharge current pulse and to slow down the plasma. When manipulating the capacitor bank voltage and inductance in the system, the velocity of the plasma can be tuned anywhere from 33 km/sec to higher than 1000 km/sec. The data are shown in Fig. 11. Notice that the Jupiter entry velocity (50 km/sec) is in this velocity range.

VI. Discussion of Mission Applications

The deflagration plasma gun reported previously was designed for high-energy plasma production and injection.[1] The application to space missions is obvious from its high specific impulse and high thrust capability. High specific impulse is not necessarily a goal for space missions, if there is no power supply to match the performance. Some adjustments were made to lower the specific impulse, since the gun performance would be matched to conventional power supplies. Pulsed operation of the gun has the disadvantage that the average thrust with time is low and the neutral gas leakage during the off period makes the specific impulse low. This can be improved if a large discharge pulse period and a fast enough open and close valve were used such that every neutral particle is processed by the deflagration discharge. The pulsed operation does have the advantage of using a pulse-network power supply to instantaneously deliver higher power for a short time with less weight than conventional steady

Fig. 9 Result of impact by plasma after one shot.

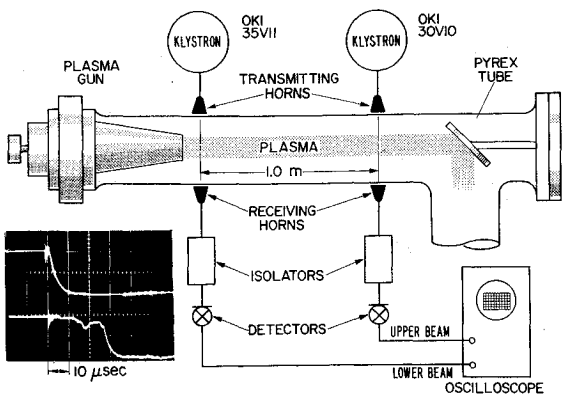

Fig. 10 Microwave time of flight measurement setup.

state power supplies. The pulsating time can be used for orbit control with telemetric c.w. (continuous waves) signals. This is very important in deep space missions, because most of the radio signals will be dispersed by the space plasma. Signal-to-noise ratio is very crucial in the control of the deep space orbiters. The neutral gas leakage can be stopped with some research effort. Therefore, it is felt, the deflagration plasma gun has a great potential to be developed as a space propulsion device. A review of the current status of all propulsion devices can be seen in Fig. 12 (Refs. 10–13). The deflagration plasma has filled the gap in the performance chart for the high specific impulse and high thrust density region. In single shot operation, its thrust density is comparable with that of chemical rockets and its specific impulse can be higher than those of current ion engines.

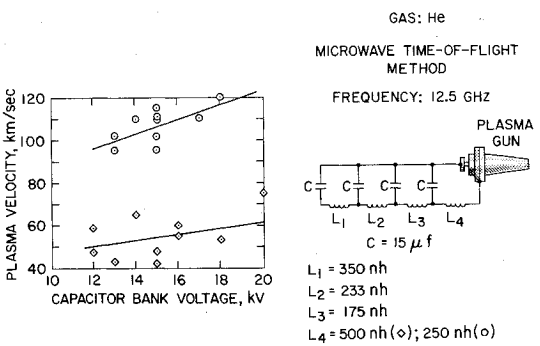

Fig. 11 Velocity front with different inductance in capacitor bank.

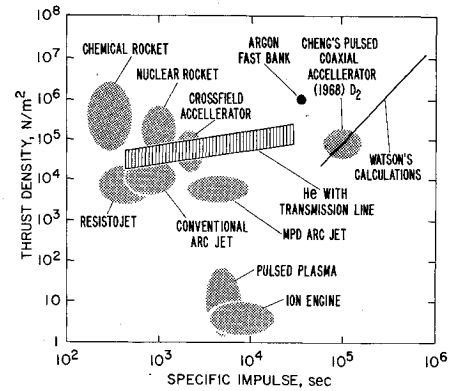

Fig. 12 A set of the specific impulse and the thrust density of all propulsion devices.

References

[1] Cheng, D. Y., "Plasma Deflagration and the Properties of a Coaxial Plasma Deflagration Gun," *Nuclear Fusion*, Vol. 10, No. 3, 1970, pp. 305–317.

[2] Lewis, B. and Von Elbe, G., *Combustion, Flame, and Explosions of Gases*, Academic Press, New York, 1961.

[3] Morozov, A. I., "Stationary Plasma Flow with Compression," *Zhurnal Tekhnicheskoi Fiziki*, Vol. 12, 1968, p. 1880.

[4] Mather, J. W., "Formation of a High-Density Deuterium Plasma Focus," *The Physics of Fluids*, Vol. 8, 1965, p. 366.

[5] Corbine, D., *Gaseous Conductor*, Dover, New York, 1958.

[6] Jahn, R. G., Clark, K. E., O'Berth, R. C., and Turchi, P. J., "Acceleration Patterns in Quasi-Steady MPD Arcs," *AIAA Journal*, Vol. 9, No. 1, Jan. 1971, pp. 167–172.

[7] Glasstone, S. and Lovberg, R., *Controlled Thermonuclear Reactions*, Van Nostrand, Princeton, N. J., 1959.

[8] Samon, J. A. R., *Techniques of Vacuum Ultraviolet Spectroscopy*, Wiley, New York, 1967.

[9] Huddlestone, R. H. and Leonard, S. L., eds., *Plasma Diagnostic Techniques*, Academic Press, New York, 1969.

[10] Watson, V. R., "Computer Simulation of a Plasma Accelerator," Ph. D. thesis, May 1969, Inst. for Plasma Research, Stanford Univ., see also "A Collisionless Model for High Specific Impulse Accelerators," AIAA Paper 69-278, Williamsburg, Va., 1969.

[11] John, R. G., *Physics of Electric Propulsion*, McGraw-Hill, New York, 1968.

[12] Mickelson, W. R. and Kaufman, H. R., "Status of Electrostatic Thrusters for Space Propulsion," TN D-2172, May 1964, NASA.

[13] Shepard, C. E., Ketner, D. M., and Vorreiter, J. W., "A High Enthalpy Plasma Generator for Entry Heating Simulation," TN D-4583, 1968, NASA.